

Carotenoid and Bacteriochlorophyll Energy Transfer in the B808–866 Complex from *Chloroflexus aurantiacus*[†]

Gabriel A. Montaña, Yueyong Xin, Su Lin, and Robert E. Blankenship*

Department of Chemistry & Biochemistry, Arizona State University, Tempe, Arizona 85287-1604

Received: May 11, 2004

The B808–866 light-harvesting complex of the filamentous anoxygenic phototrophic green bacterium *Chloroflexus aurantiacus* has characteristics of both the LH1 and LH2 antenna complexes found in purple photosynthetic bacteria. Energy transfer kinetics in this complex were studied using ultrafast transient absorption spectroscopy and time-resolved fluorescence spectroscopy, including the excited singlet states of the γ -carotene present in the B808–866 complex and energy transfer to the B866 Bchl *a*. Energy transfer from the carotenoid S₁ state to the B866 Bchl *a* was observed and found to be ~12–15% efficient. A separate pathway, populating the previously described S* state, was also observed as a precursor to carotenoid triplet state formation. While the energy transfer efficiency is similar to what has been reported for LH1 complexes of *Rhodospirillum rubrum*, the kinetic scheme for energy relaxation and transfer is somewhat different than that seen in either LH1 from *Rhodospirillum rubrum* or LH2 of *Rhodobacter sphaeroides*.

Introduction

In photosynthesis, light-harvesting complexes effectively capture energy in the form of photons and pass this energy to the reaction center complex where photochemistry takes place. Carotenoids have been determined to play fundamental roles in light-harvesting complexes, both by absorbing and transferring energy and also by quenching harmful bacteriochlorophyll triplet and singlet oxygen states.¹

In carotenoids, the optical transition from the ground state, S₀ to the first excited state, S₁, is symmetry forbidden, while that to the second excited singlet state, S₂, is symmetry allowed.¹ Therefore, the strong blue absorption characteristic of carotenoids is due to population of the S₂ state. Rapid internal conversion then takes place from the S₂ state to the S₁ state on the order of 200 fs and subsequent relaxation to the ground state on the picosecond time scale.

Recent evidence has suggested the presence of more carotenoid excited states that can be observed in isolated β -carotene, spirilloxanthin (Spx), and purple bacterial light-harvesting complexes.^{1–3} The so-called 1Bu[–] state has been theoretically proposed for years, and recent evidence has proposed that it is populated by an ultrafast relaxation on the time scale of 50 fs from the 1Bu⁺(S₂) state and decays to form the 2Ag[–](S₁) state.⁴ A second pathway with a picosecond lifetime that has been proposed as a pathway to triplet state formation has also been observed and has been termed the S* state.^{3,5} This has also been observed to be a singlet state and has previously been described as a possible 1Bu state.³

In photosynthetic antennae, energy transfer to subsequent bacteriochlorophyll or chlorophyll molecules must out-compete rapid relaxation processes in order for the carotenoids to contribute significantly to the light harvesting. This efficiency of energy transfer has been seen to vary from species to species as well as from complex type to type.⁶ In LH2 complexes of *Rhodobacter sphaeroides*, energy transfer efficiency is >90%

and has been observed from the S₂, S₁, and S* states.⁵ The ability to transfer energy from all three of these states has been implicated in creating the efficient energy transfer process. In the LH1 complexes of *R. rubrum*, energy transfer efficiency from the carotenoids to the Bchl *a* is much less, on the order of 35%. Only energy transfer from the S₂ state is observed, thereby contributing to the low efficiency of energy transfer.³

Chloroflexus aurantiacus is a green thermophilic photosynthetic bacterium containing a membranous photosynthetic architecture similar to purple bacteria⁷ and peripheral chlorosome antenna complexes unique to green and filamentous anoxygenic phototrophic (FAP) bacteria.⁸ Experimental evidence has shown sequential downhill energy transfer from the chlorosomes to the B808–866 complex via the baseplate and into the reaction center.^{8–10} Trapping by the P870 reaction center occurs in ~200 ps in oxidized reaction centers^{10,11} and in ~70 to 90 ps in reduced reaction centers.¹⁰

The B808–866 complex of *C. aurantiacus* is spectrally most similar to the purple bacterial LH2 complex. It has two types of Bchl *a* absorbing chromophores at 808 and 866 nm, respectively. The relative ratios of the 808 to 866 nm peaks are also similar to those observed in LH2 complexes with the more pronounced peak arising from the longer wavelength 866 nm absorbing region. However, the α - and β -peptides show higher sequence similarity to the α - and β -peptides of the LH1 complexes and show less similarity to the LH2 peptides.^{12,13} Whether the B808–866 complex surrounds the reaction center such as is postulated in LH1 complexes or forms smaller rings typical of LH2 complexes is not known. There is no evidence from biochemical, spectroscopic data or from the *Chloroflexus* genome for authentic LH2 complexes in this organism.

In this study, we examined the B808–866 carotenoid energy transfer processes as well as the B808 to B866 energy transfer. Ultrafast time-resolved spectroscopy was used to monitor the γ -carotene relaxation kinetics as well as the carotenoid to bacteriochlorophyll energy transfer processes. A kinetic model of carotenoid energy transfer within the B808–866 complex

[†] Part of the special issue "Gerald Small Festschrift".

* Corresponding author. Phone: (480) 965-4430. Fax: (480) 965-2747.

has been developed, and comparisons are made to the LH1 and LH2 complexes of purple bacteria.

Materials and Methods

B808–866 Reaction Center Isolation. A procedure modified from that of Feick and Fuller¹⁴ for isolating the B808–866 complex was used in these studies. *C. aurantiacus* cells were resuspended in a 2 M NaSCN/10 mM phosphate/10 mM ascorbic acid buffer, pH 7.4, homogenized, and broken in a French press at 20 000 psi. The membranes were pelleted by centrifugation at $12\,500 \times g$ for 20 min, subjected to detergent extraction with 20% cholic acid, and incubated at 37 °C for 6 h. The sample was centrifuged at $266\,000 \times g$ for 2 h and the pellet collected. The pellet was resuspended in 10 mM phosphate buffer, pH 7.4, dialyzed against 10 mM phosphate buffer, pH 7.4, to remove any detergent, and stored at 4 °C. The presence of B808–866 proteins as well as RC proteins was determined by SDS–PAGE. The activity of the RC complex in samples was determined by light–dark absorption difference spectroscopy.

Steady-State Transmission and Fluorescence Spectroscopy. (1-T) transmission spectra were taken using a Shimadzu UV-2501PC spectrophotometer with a 2 nm spectral bandwidth. Steady-state fluorescence spectra were taken using a 4 nm spectral bandwidth on a Photon Technology International (PTI) fluorimeter with an Advanced Photonics Inc. avalanche photodiode detector. Fluorescence excitation spectra were obtained with emission monitored at 885 nm and emission spectra with excitation at 465 nm.

Ultrafast Spectroscopy. Femtosecond transient absorption spectroscopy (TAS) was performed using a pump–probe setup described previously.¹⁵ For carotenoid energy transfer processes the sample was excited at 482 nm with 100 fs pulses at a repetition rate of 1 kHz. The absorbance changes were recorded between 490 and 740 nm as well as between 770 and 1060 nm with a 2 nm wavelength resolution. For B808 to B866 nm energy transfer processes the sample was excited at 800 nm with 100 fs pulses at a repetition rate of 1 kHz. The absorbance changes were recorded between 770 and 910 nm with a 2 nm wavelength resolution. Laser excitation of 2 mW was used, and the polarization was set at a magic angle relative to that of the probe beam. Global analysis was performed on the data to obtain decay-associated spectra.

Picosecond fluorescence decays were recorded on a single-photon counting apparatus. Measurements were performed until 10 000–20 000 counts were accumulated in the peak channel. A channel resolution of 6.5 ps was used. The fluorescence decays were detected at several emission wavelengths. The sample was excited by a cavity-dumped dye laser at a wavelength of 598 nm. The fluorescence decay data were analyzed by global analysis methods employing a sum of exponentials as the model function. The quality of the fits was judged by individual or global χ^2 values as well as by residual plots.

Results and Discussion

Figure 1 shows a steady-state (1-T) transmission and fluorescence profile of the B808–866 complex. The complex has two prominent peaks in the near-IR at 808 and 866 nm, respectively, strong absorption in the visible region due to carotenoid absorption, as well as contribution from the Bchl *a* Soret region. Absorption at 670 nm is due to residual Bchl *c* as well as a small contribution from the reaction center. As can be observed, the peaks at 808 and 866 nm are in similar ratios

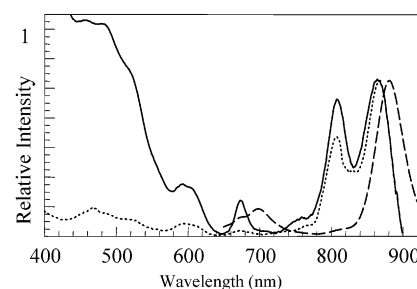


Figure 1. Transmission (1-T) and fluorescence spectra of the isolated B808–866 light-harvesting complex from *C. aurantiacus*. The (1-T) spectrum (—) shows two distinct peaks in the near-IR at 808 and 866 nm, respectively, as well as *Qx* Bchl *a* absorption at ~600 nm and reaction center complex (or free Bchl *c*) at 670 nm. The absorption in the visible blue region is due to Soret absorption by Bchl *a* as well as contribution from γ -carotene present in the complex. The fluorescence emission spectrum (---) shows strong emission centered at 875 nm with excitation at 465 nm. The excitation spectrum (···) monitored at 885 nm exhibits ~12% carotenoid to B866 energy transfer as well as more than 80% B808 to B866 nm energy transfer.

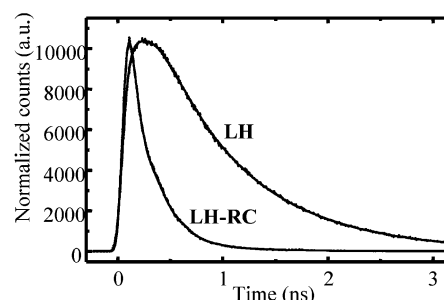


Figure 2. Fluorescence kinetics of B808–866 complex with and without reaction centers, recorded at 865 nm. The smooth lines are theoretical fitting curves. See Table 1 for fitting parameters.

TABLE 1: Fluorescence Lifetimes and Amplitudes Obtained by Analyzing the Data with Global Analysis

	τ_1 ns	A1 %	τ_2 ns	A2 %	τ_3 ns	A3 %	τ_4 ns	A4 %
LH	0.004	−1.8	0.21	19.4	0.832	76.85	1.85	1.67
LH + RC	0.05	74.5	0.154	22.9	0.602	1.45	1.98	1.15

as those observed in LH2 complexes and the overall spectrum resembles that of LH2 complexes, however with higher absorbance in the visible blue region. The fluorescence emission spectrum indicates energy transfer to the B866 Bchl *a* molecules upon excitation at 465 nm. The spectra are indicative of energy transfer to the lower energy B866 Bchl *a* with no observable emission from the B808 Bchl *a*, similar to observations in LH2-type complexes. The fluorescence excitation spectrum shows nearly complete energy transfer from the B808 to the B866 Bchl *a* as well as ~12% energy transfer from the carotenoids, which exhibit visible absorption in the 450–500 nm range, to the B866 Bchl *a* molecules.

The excited-state lifetimes of the B808–866 complex were characterized using single-photon counting fluorescence spectroscopy.⁹ Figure 2 shows the fluorescence kinetic traces recorded at 865 nm for the B808–866 complex with and without the reaction center. The fitting results using four decay components are listed in Table 1. Without the reaction center, the B808–866 complex decays with two major lifetimes of 210 ps (19.4%) and 832 ps (77%). The dominant decay lifetime of 830 ps agrees with published data.¹⁶ The 210 ps component is thought to be due to some contamination of the oxidized reaction centers present in the sample. When the reaction center is present the major decay lifetime component of 50 ps (75%) is consistent

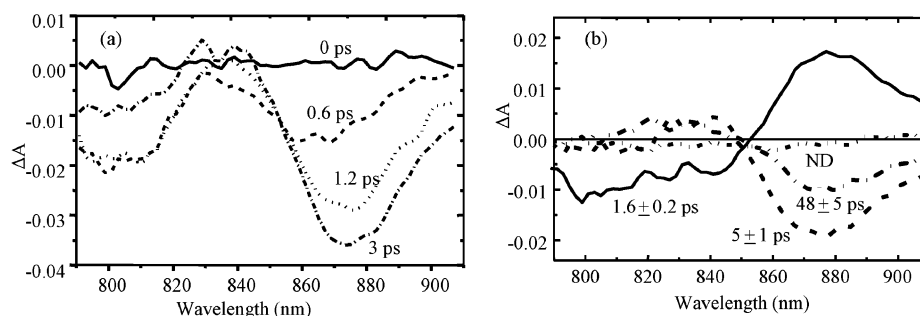


Figure 3. Near-IR transient absorption spectra and decay-associated spectra of B808–866. (a) Transient absorption spectra show rapid energy transfer from B808 to B866 Bchl *a* upon direct excitation into the B808 Bchl *a* at 800 nm. Nearly complete energy transfer is observed within 3 ps. (b) Decay-associated spectra indicating a 1.6 ± 0.2 ps energy transfer process from the B808 Bchl *a* to the B866 Bchl *a*. Lifetimes of 5 ± 1 ps, 48 ± 5 ps, and an ND component for the B866 Bchl *a* are also obtained from the fitting.

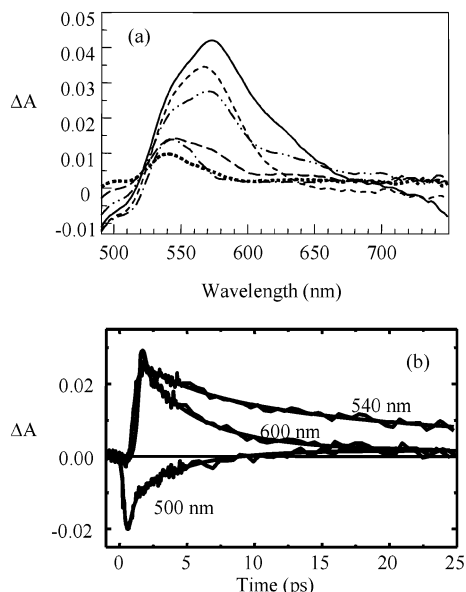


Figure 4. Transient absorption spectra and kinetics of the visible carotenoid region of the B808–866 complex. (a) TAS show quick energy transfer from the excited S_2 state to the S_1 state within 1.23 ps (— · —) and the evolution of the spectra with times given at 1.9 ps (— · —), 2.10 ps (—), 4.0 ps (— · —), 10 ps (— · —), and 20 ps (· · ·) which shows remaining absorption centered at ~ 530 nm. (b) Kinetics monitored at three different wavelengths indicating recovery of S_2 (500 nm) absorption, decay of the S_1 (600 nm) state, and the long-lived nature of the S^* state (540 nm).

with the presence and trapping by reduced reaction centers.¹⁷ The 154 ps decay component (23%) is postulated to be due to the reduced reaction center as previously described.

The energy transfer processes occurring within and between the Bchl *a* molecules are displayed in Figure 3. The transient absorption spectra in Figure 3a between 790 and 910 nm show the rapid energy transfer from the B808 Bchl *a* to the B866 Bchl *a* upon direct excitation into the former at 800 nm. The TAS shows almost immediate delocalization followed by a rapid energy transfer to the B866 nm Bchl *a*. There is also a progressive excitation relaxation in the B866 nm region as well as the buildup of stimulated emission in the B866 nm region to a final center of ~ 875 nm within 3 ps. The DAS spectra in Figure 3b indicate an energy transfer process with a time constant of 1.6 ps from the B808 to the B866 nm Bchl *a* molecules. A 5 ps decay component centered at 875 nm is also observed and attributed to ultrafast trapping by the reaction center. A 48 ps component centered at 875 nm is also observed and is consistent with the reaction center quenching observed by SPC. A nondecaying (ND) component is observed and is

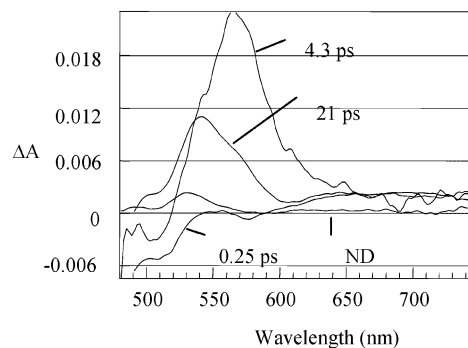


Figure 5. Decay-associated spectra of the visible carotenoid region upon excitation at 482 nm. The 0.25 ps component is due to a combination of absorption recovery of the S_2 state and the buildup of S_1 to S_N absorption increase signal. The 4.3 ps component is attributed to the decay lifetime of the S_1 state, the 21 ps component is attributed to the S^* state decay lifetime, and the ND component is attributed to the carotenoid triplet state formed.

attributed to the slower processes presented in the SPC data that are not resolvable by picosecond TAS.

Figure 4 shows the transient absorption spectra and kinetics associated with the visible region of the carotenoid spectrum. With excitation at 482 nm, rapid relaxation to the S_1 state is followed by the observed S_1 to S_N absorption centered at 579 nm within 1 to 2 ps. Any faster energy conversion processes, such as molecular relaxation,¹⁸ are not resolved. By 1.9 ps, the center of absorbance shifts to 562 nm with a large decrease in absorbance to the red side of the spectrum. At 4.0 ps, the distinct appearance of two separate peaks at ~ 565 nm and ~ 535 nm is visible. The former decays rapidly and by 10 ps appears as a shoulder to the 535 nm absorbance peak. This absorbance is still observed at 20 ps. The kinetics in Figure 4b show the decay components associated with three different carotenoid processes. The kinetic trace at 500 nm shows the bleaching and recovery of the ground state. The nondecaying nature of the 540 nm absorption is attributed to the triplet state formed from the S^* state. The kinetics for the S^* state component create the biphasic nature of the 540 nm kinetic trace. The kinetic trace at 600 nm is consistent with S_1 – S_0 decay.

Figure 5 shows decay-associated spectra (DAS) associated with the visible carotenoid absorption fit with four kinetic components. The negative signal in the 0.25 ps spectrum is due to S_2 stimulated emission (SE) as well as excited-state absorption greater than 590 nm. The 4.3 ps component is assigned to relaxation of the S_1 state to its ground state. This time is shortened compared to isolated γ -carotene in organic solvent due to energy transfer to the B866 Bchl *a* molecules² as will be discussed later. The 21 ps component with its center wavelength at 539 nm is assigned to the S^* state decay observed

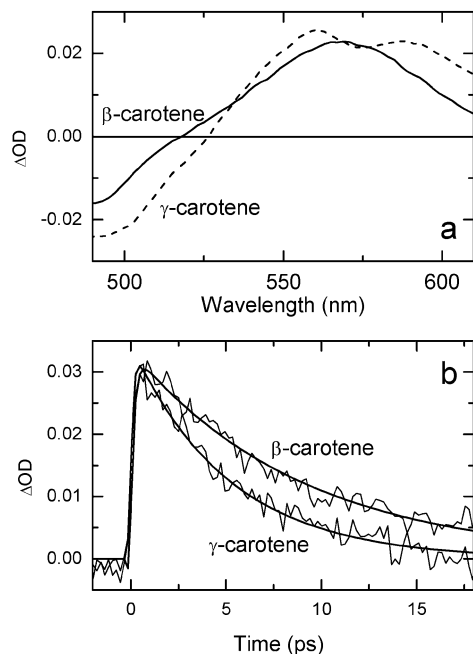


Figure 6. (a) Time-resolved spectra of β -carotene (solid line) and γ -carotene (dashed line) in methanol, recorded at 1 ps after laser excitation at 480 nm. (b) Kinetic traces of the S_1 to S_0 transition of β -carotene at 570 nm (upper lines) and γ -carotene at 560 nm (lower lines) with a two-exponential fit (see text for lifetimes).

by previous groups.^{3,5} The nondecaying component centered at 530 nm is thought to be due to the long-lived triplet state formed from the S^* state.

Figure 6 shows TAS and kinetic fits of both γ - and β -carotene for comparison. Figure 6a shows TAS of both carotenoids in methanol at 1 ps. Figure 6b shows the kinetic traces and fits indicating a 0.18 ps rise and 8.92 ps decay for β -carotene and a 0.12 ps rise and 5.1 ps decay for γ -carotene. The values observed for β -carotene agree with previously reported values, therefore, we are confident in the components generated for γ -carotene.

Figure 7 shows transient absorption spectra and kinetics observed in the B808–866 nm absorbing region after excitation of carotenoids. Upon excitation at 482 nm a bleaching in absorption is observed within 1 ps at the 866 nm absorption region as well as an absorption increase centered at around 890 nm. Maximum bleaching at the B866 nm region is reached within 1.5 ps and does not decay within the time measured (25 ps). The long wavelength absorption, which broadens between 880 and 1050 nm, decays almost completely within 2 ps. Absorbance in this 880–1050 nm region has been reported to be due to carotenoid 1Bu⁺ absorption, although whether it is due to 1Bu⁺ or the previously reported 1Bu⁻ state^{2,19} or a combination of the two is not resolvable. Bleaching of the B866 nm absorption is complete within 2 ps.

The overall energy scheme determined from these studies is presented in Figure 8. Upon initial excitation to the S_2 state, energy relaxation to both the S^* state and S_1 state occurs within 250 fs. The S_2 energy transfer contribution is not resolvable and will not be discussed further. Energy transfer to the B866 Bchl *a* from the S_1 state then occurs within a few picoseconds. Maximum bleaching is reached within 1.5 ps; therefore, no indication of energy transfer from the S^* state to the B866 nm region is detected. The lifetime of the S_1 – S_n excited-state absorption, 4.3 ps, indicates a roughly 16% energy transfer from the carotenoid S_1 state to the B866 nm Bchl *a*. To determine the overall energy transfer efficiency, the amount of S_1

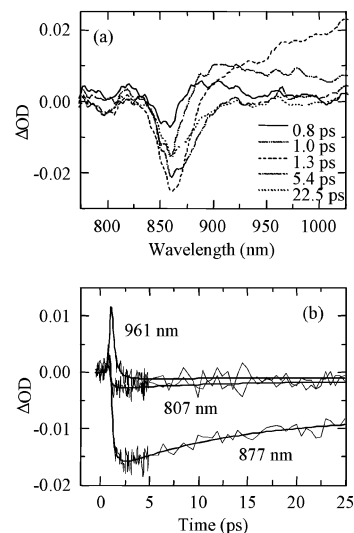


Figure 7. Transient absorption spectra and kinetics for the near-IR region of B808–866 with 482 nm excitation. (a) TAS shows absorption bleaching centered at 860 nm at 0.85 ps (—), followed by further bleaching as well as absorption increase at wavelengths greater than 890 nm by 1.02 ps (— · —) that maximizes by 1.34 ps (---). The decay of the long wavelength absorption as well as bleaching recovery centered around the B866 nm region are presented in the remaining spectra at times 5.42 ps (— · —) and 22.5 ps (· · ·). (b) Kinetic traces at 807, 877, and 961 nm.

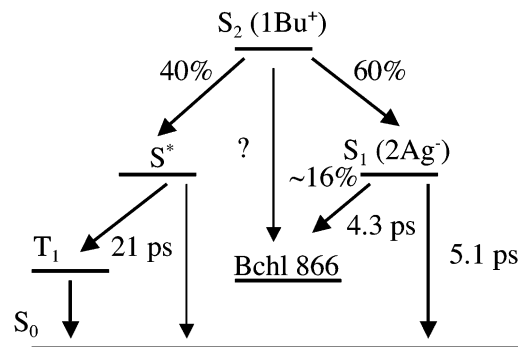


Figure 8. Kinetic scheme for carotenoid energy transfer in the B808–866 complex.

population from S_2 excitation must first be determined. By integration of the area under the S^* and S_1 DAS, it can be estimated that roughly 60% of the S_2 excitation relaxes to the S_1 state. Given the 16% energy transfer from the S_1 state to the B866 Bchl *a*, as noted above, the estimated percent of energy transfer from the carotenoid to the Bchl should be ~9%. As has been noted earlier in the excitation spectrum, ~12% energy transfer is observed. This would indicate that little to no energy transfer occurs from any of the other carotenoid pathways. There exists the possibility that a small amount of energy transfer from the S_2 state to Bchl *a* may occur; however, we are unable to resolve this with our decay lifetimes. The S^* state which is seen as excited-state absorption centered at 539 nm has a decay lifetime of 21 ps. This time is considerably longer than that observed in either LH1 or LH2 studies;^{3,5} however, its shape is consistent with it being the S^* state previously reported. The nondecaying component observed is interpreted as being triplet state formation.

The carotenoid energy transfer mechanism presented here once again points to the unique hybrid nature of the B808–866 complex. It has a low level of energy transfer from its carotenoid species and appears to undergo primarily S_1 to Bchl *a* energy transfer. Efficient energy transfer from the S_2 state as

well as from the S^* state have been implicated in describing the >90% energy transfer observed in some LH2 complexes.⁵ The energy transfer in the B808–866 complex appears on the other hand to be different from either the LH2 or LH1 complexes. In the LH1 complex of *R. rubrum* energy transfer is observed from the S_2 state only, and this is used to explain its low energy transfer efficiency.³

How to ascribe the S^* energy level is not clear. The findings of Koyama's group as well as recently published findings,⁴ indicate that the previously proposed $1Bu^-$ state may indeed be an intermediate of energy transfer between the S_2 state and the S_1 state and have a lifetime on the order of ~50 fs. This would indicate that the S^* state observed in these studies and described previously is not the $1Bu^-$ state but instead a separate singlet state. It also has been shown to not be a triplet state or due to the S_1 state absorption.³ The findings in this study indicate population of the S^* state at the same time as S_1 population and a lifetime longer than that of the S_1 state. Therefore, it is not possible to describe the S^* state as a pathway to S_1 population. It appears to exist primarily as a pathway to long-lived triplet state formation. Faster time-resolved experiments are necessary to fully understand and complete the energetic landscape present in the B808–866 complex.

As described earlier, the B808–866 complex appears to be genetically similar to LH1 complexes while spectrally resembling the LH2 complexes of purple bacteria. However, the energy transfer pathway observed, through S_1 alone, is different from either the LH2 or LH1 complexes studied. Studies on the LH1 complex of *R. rubrum* reported energy transfer through the S_2 , S_1 , and S^* states. Since the B808–866 complex is by sequence comparisons similar to this complex, it is possible that its evolutionary modifications have altered the energy transfer properties from the S_2 and S^* state while maintaining the ability to transfer energy from the S_1 state to Bchl *a*. Likewise, the energy transfer from the B808 to the B866 nm Bchl *a* is much slower than that observed in LH2 complexes from purple bacteria, indicating further differences between the B808–866 complex and LH2 complexes. It must also be considered that although it spectrally resembles LH2 complexes, the B808–866 complex exists as the primary light-harvesting complex associated with the reaction center. Initial studies have shown it to exist as a ring structure around the reaction center, however, with a diameter of >20 nm, twice the size of the LH1 complexes previously observed.²⁰

Conclusions

In this paper we present a description of the carotenoid energy transfer pathways within the B808–866 light-harvesting complex from *Chloroflexus aurantiacus*. The carotenoid relaxation kinetics as well as the energy transfer pathway to Bchl *a* proved to be uniquely different from those observed in either LH1 or LH2 complexes

The results presented also give further evidence to the presence of the S^* state. Although the lifetime observed is substantially longer than previously observed measurements in LH complexes in purple bacteria, its shape and apparent rise to triplet state formation is indicative of its presence. The studies presented here give further insight to the unique organization of the B808–866 complex. In order to fully characterize this system, further spectroscopic, microscopic, and structural analyses are necessary. Due to its unique makeup, significant questions dealing with the evolution of light-harvesting complexes as well as energy transfer processes can be addressed with further studies of this system.

References and Notes

- (1) Koyama, Y.; Hashimoto, H. In *Carotenoids in Photosynthesis*; Young, A., Britton, G., Eds.; Chapman and Hall: London, 1993; p 327.
- (2) Zhang, J.; Fujii, R.; Koyama, Y.; Rondonuwu, F.; Watanabe, Y.; Mortensen, A.; Skibsted, L. *Chem. Phys. Lett.* **2001**, *348*, 235.
- (3) Gradinaru, C.; Kennis, J.; Papagiannakis, E.; van Stokkum, I.; Cogdell, R.; Fleming, G.; Niederman, R.; van Grondelle, R. *Proc. Natl. Acad. Sci. U.S.A.* **2001**, *98*, 2364.
- (4) Cerullo, G.; Polli, D.; Lanzani, G.; De Silvestri, S.; Hashimoto, H.; Cogdell, R. *Science* **2002**, *298*, 2395.
- (5) Papagiannakis, E.; Kennis, J.; van Stokkum, I.; Cogdell, R.; van Grondelle, R. *Proc. Natl. Acad. Sci. U.S.A.* **2002**, *99*, 6017.
- (6) Frank, H.; Cogdell, R. J. In *Carotenoids in Photosynthesis*; Young, A., Britton, G., Eds.; Chapman and Hall: London, 1993; p 252.
- (7) Thornber, J.; Cogdell, R.; Pierson, B.; Seftor, R. J. *Cell. Biochem.* **1983**, *23*, 159.
- (8) Blankenship, R. E.; Olson, J. M.; Miller, M. Antenna Complexes from Green Photosynthetic Bacteria. In *Anoxygenic Photosynthetic Bacteria*; Blankenship, R. E., Madigan, M. T., Bauer, C. E., Eds.; Kluwer Academic Publishers: Dordrecht, 1995; p 399.
- (9) Causgrove, T. P.; Brune, D. C.; Wang, J.; Wittmershaus, B. P.; Blankenship, R. E. *Photosynth. Res.* **1990**, *26*, 39.
- (10) Muller, M.; Griebenow, K.; Holzwarth, A. *Biochim. Biophys. Acta* **1993**, *1144*, 161.
- (11) Mimuro, M.; Nozawa, T.; Tamai, N.; Shimada, K.; Yamazaki, I.; Lin, S.; Knox, R.; Wittmershaus, B.; Brune, D.; Blankenship, R. J. *Phys. Chem.* **1989**, *93*, 7503.
- (12) Wechsler, T. D.; Brunisholz, R. A.; Frank, G.; Suter, F.; Zuber, H. *FEBS Lett.* **1987**, *210*, 189.
- (13) Zuber, H.; Cogdell, R. J. Structure and Organization of Purple Bacterial Antenna Complexes. In *Anoxygenic Photosynthetic Bacteria*; Blankenship, R. E., Madigan, M. T., Bauer, C. E., Eds.; Kluwer Academic Publishers: Dordrecht, 1995; p 315.
- (14) Feick, R. G.; Fuller, R. C. *Biochemistry* **1984**, *23*, 3693.
- (15) Melkozernov, A. N.; Lin, S.; Blankenship, R. E. *Biochemistry* **2000**, *39*, 1489.
- (16) Griebenow, K.; Muller, M. G.; Holzwarth, A. R. *Biochim. Biophys. Acta* **1991**, *1059*, 226.
- (17) Nuijs, A. M.; Vasmel, H.; Duysens, L. N. M.; Amesz, J. *Biochim. Biophys. Acta* **1986**, *849*, 316.
- (18) de Weerd, F.; van Stokkum, I.; van Grondelle, R. *Chem. Phys. Lett.* **2002**, *354*, 38.
- (19) Sashima, T.; Nagae, H.; Kuki, M.; Koyama, Y. *Chem. Phys. Lett.* **1999**, *299*, 187.
- (20) Karrasch, S.; Bullough, P.; Ghosh, R. *EMBO J.* **1995**, *14*, 631.